PB86-167731

Measurement and Prediction of Single Droplet Trajectories in a Swirled Combustion System

Acurex Corp., Research Triangle Park, NC

Prepared for

Environmental Protection Agency
Research Triangle Park, NC

Mar 86

U.S. Department of Commerce
National Technical Information Service
NTIS

PB86-167731

EPA/600/D-86/049
March 1986

MEASUREMENT AND PREDICTION OF SINGLE DROPLET TRAJECTORIES IN A SWIRLED COMBUSTION SYSTEM

J. A. Mulholland
U.S. Environmental Protection Agency
Air and Energy Engineering Research Laboratory
Research Triangle Park, NC 27711

R. K. Srivastava and J. V. Ryan
Acurex Corporation
Research Triangle Park, NC 27709

S. B. Robinson and W. S. Lanier
Energy and Environmental Research Corporation
Chapel Hill, NC 27514

J. O. L. Wendt
University of Arizona
Tucson, AZ 85721

AIR AND ENERGY ENGINEERING RESEARCH LABORATORY
OFFICE OF RESEARCH AND DEVELOPMENT
U.S. ENVIRONMENTAL PROTECTION AGENCY
RESEARCH TRIANGLE PARK, NC 27711

REPRODUCED BY
NATIONAL TECHNICAL
INFORMATION SERVICE
U.S. DEPARTMENT OF COMMERCE
SPRINGFIELD, VA. 22161

TECHNICAL REPORT DATA
(Please read Instructions on the reverse before completing)

1. REPORT NO.	2.	3. RECIPIENT'S ACCESSION NO.
EPA/600/D-86/049		PB86 167731/AS

4. TITLE AND SUBTITLE	5. REPORT DATE
Measurement and Prediction of Single Droplet Trajectories in a Swirled Combustion System	March 1986
	6. PERFORMING ORGANIZATION CODE
7. AUTHOR(S) J. A. Mulholland (EPA), R. K. Srivastava and J. V. Ryan (Acurex), S. B. Robinson and W. S. Lanier (EERC), and J. O. L. Wendt (Univ. of Arizona)	8. PERFORMING ORGANIZATION REPORT NO.
9. PERFORMING ORGANIZATION NAME AND ADDRESS (1) Acurex Corp., Research Triangle Park, NC 27709. (2) Energy and Environmental Research Corp., Chapel Hill, NC 27514	10. PROGRAM ELEMENT NO.
	11. CONTRACT/GRANT NO. (1) 68-02-3988. (2) 68-02-4247.
12. SPONSORING AGENCY NAME AND ADDRESS EPA, Office of Research and Development, Air and Energy Engineering Research Laboratory, Research Triangle Park, NC 27711	13. TYPE OF REPORT AND PERIOD COVERED Published Paper; 10-12/85
	14. SPONSORING AGENCY CODE EPA/600/13

15. SUPPLEMENTARY NOTES AEERL project officer is James A. Mulholland, Mail Drop 65, 919/541-7663.

16. ABSTRACT The paper gives results of an experimental determination of the penetration of individual fuel droplets injected into a swirling gas flame, as a function of the droplet injection parameters of spacing, velocity, size, and angle. It also describes additional experiments in cold flow to evaluate the effect of droplet spacing on drag coefficient. Theoretical predictions of a simplified three-dimensional droplet trajectory model compared well to the hot flow experimental observations. It was found that bypassing and penetration of large droplets, which can occur in practical situations, may lead to failures in liquid-fired hazardous waste incinerators. Cold flow studies indicated that the average drag coefficient depended strongly on droplet spacing, for a droplet spacing of less than 150 droplet diameters. Although turbulent fluctuations gave rise to distributions of droplet paths, both their average behavior and their trends with respect to injection variables compared well to trajectory predictions utilizing the experimentally determined mean velocity field.

17. KEY WORDS AND DOCUMENT ANALYSIS

a. DESCRIPTORS	b. IDENTIFIERS/OPEN ENDED TERMS	c. COSATI Field/Group
Pollution, Aerodynamics, Combustion, Flames, Drops (Liquids), Trajectories, Measurement, Predictions	Pollution Control, Stationary Sources	13B, 20D, 21B, 07D, 19D, 14B, 14G

18. DISTRIBUTION STATEMENT	19. SECURITY CLASS (This Report)	21. NO. OF PAGES
Release to Public	Unclassified	28
	20. SECURITY CLASS (This page) Unclassified	22. PRICE

EPA Form 2220-1 (9-73)

NOTICE

This document has been reviewed in accordance with U.S. Environmental Protection Agency policy and approved for publication. Mention of trade names or commercial products does not constitute endorsement or recommendation for use.

MEASUREMENT AND PREDICTION OF SINGLE DROPLET TRAJECTORIES IN A SWIRLED COMBUSTION SYSTEM

J. A. Mulholland
U.S. Environmental Protection Agency

R. K. Srivastava and J. V. Ryan
Acurex Corporation

S. B. Robinson and W. S. Lanier
Energy and Environmental Research Corporation

J. O. L. Wendt
University of Arizona

ABSTRACT

The penetration of individual fuel droplets injected into a swirling gas flame was determined experimentally as a function of the droplet injection parameters of spacing, velocity, size and angle. Additional experiments in cold flow were performed to evaluate the effect of droplet spacing on drag coefficient. Theoretical predictions of a simplified three-dimensional droplet trajectory model, which utilized measured temperature and velocity fields, compared well to the hot flow experimental observations. It was found that bypassing and penetration of large droplets can occur in practical situations and that this may lead to possible failure modes in liquid-fired hazardous waste incinerators.

The 100 kW gas flames were supported on a movable-block swirl burner mounted on a 50 cm diameter horizontal combustor. Detailed temperature and velocity fields were measured using suction thermocouples and a calibrated five-hole pitot tube. The droplet generator, which was of the vibrating orifice type, produced a monodisperse stream of equally spaced droplets, which was injected at an angle into the combustor flow field. Cold flow studies indicated that the average drag coefficient depended strongly on droplet spacing, for a droplet spacing of less than 150 droplet diameters.

A theoretical three-dimensional droplet trajectory and evaporation model was used to solve the uncoupled equations of droplet motion in a Lagrangian framework. Although turbulent fluctuations gave rise to distributions of droplet paths, both their average behavior and their trends with respect to injection variables compared well to trajectory predictions utilizing the experimentally determined mean velocity field. In order to determine the probability of single droplet penetration, however, future work must address the interaction between turbulent fluctuations and droplet paths. Additional work is also required to quantify the effect of droplet spacing on droplet drag in a hot three-dimensional flow field.

INTRODUCTION

The combustion of liquid fuels in most practical swirled combustors is dominated largely by the overall dynamics of the fuel spray and by the combustion of particle clouds, rather than by the trajectories of single droplets.[1] However, in the incineration of liquid hazardous wastes, the situation is different. Here, a destruction removal efficiency (DRE) in excess of 99.99 percent is required, and the penetration or bypassing of the flame zone of a very few individual droplets can lead to a failure mode. For example, the escape of one rogue 300 μm droplet out of 2 million droplets of a mean diameter of 50 μm will lead to a DRE of less than 99.99 percent and, thus, to a failure of the incinerator. Measurements of droplet size distributions in various fuel sprays have found diameters of 100 to 500 μm, which is an order of magnitude larger than the mean.[2] These rogue droplets tend to concentrate at the outer edge of the spray core. The subsequent fate of these individual drops is then of paramount importance. This research, therefore, focuses on the measurement and prediction of trajectories of individual large droplets in hot, swirling practical combustor flow fields. The objective is, first, to determine the extent to which the behavior of a rogue droplet in a practical aerodynamic flow field can be predicted using existing models and, second, to delineate the requirements necessary for a model that can ultimately allow the relationship between large droplet injection characteristics and DRE to be determined.

Droplet burning is fundamental to many combustion systems and has received much attention.[3-5] Theoretical solutions have been derived for both single droplet and group combustion by assuming idealized combustion environments.[6,7] Thus far, however, these models, with their simplified (external) fluid mechanics, have been unsuccessful in predicting experimental results from practical combustors.[8] The present paper complements the results of others and describes the application of a simplified three-dimensional droplet trajectory and evaporation model to predict the experimentally determined behavior of large single droplets in a complex swirled combustion flow field.

This paper consists of four parts. First, the 100 kW combustion facility and the droplet generator are described in detail, and the ensuing detailed temperature and velocity maps of the baseline gas flame are presented. Second, the critical issue of the effect of droplet spacing on droplet drag coefficient is addressed in a simple cold flow experiment. Third, actual experimental droplet trajectories in the gas flame are described as functions of droplet spacing, velocity, diameter and angle. The results are then compared to calculations of mean droplet trajectories based on a model developed by Ayers et al.[8] Finally, the model is exercised to ascertain conditions at which failure in liquid-fired incinerators can occur, and future requirements for and improvements to the model are delineated.

EXPERIMENTAL

Combustor and Droplet Generator

The bench-scale combustion facility is shown in Fig. 1. The 100 kW combustor is a horizontal cylinder with a large quartz window for flame visualization and multiple ports for in-flame sampling. A movable-block swirl burner[9] with interchangeable fuel nozzles is mounted on the combustor and is capable of providing good near-burner zone aerodynamic simulation of various flame types. The front wall contains a slot to allow for off-axis droplet injection, as shown (Fig. 1).

Natural gas was burned at an excess air of 30 percent, ensuring that sufficient oxygen was available for droplet combustion. A Type C flame,[10] produced with a high combustion air swirl (S=1.3) and a 45 degree fuel nozzle, was 10 to 15 cm long and was stabilized on the burner quarl by strong primary internal recirculation of the hot combustion gases.

The droplet generator is a vibrating orifice device,[11] with ancillary electronics to facilitate droplet-to-droplet spacing variation.[12] A mixture of 80 percent (by volume) Shell fuel additive ASA-3, comprised mostly of xylene, and 20 percent distillate fuel oil was used as a nominal test liquid. This fluid was selected on the basis of conductivity (for electrostatic charging and deflection), viscosity (for droplet formation) and luminosity in the flame (for visualization). Droplet parameters varied were

spacing, size, velocity and injection angle. Spacing was varied by charging, then deflecting, every Nth droplet, with the neutral droplets being trapped and recirculated.[12] Size was varied by changing orifices, with droplet diameter found to be approximately twice the orifice diameter in these tests. Droplet diameter, D, and droplet spacing in the stream, ℓ_{ds}, were measured using a strobe light and microscope. The droplet spacing after separation, ℓ_d, is given by

$$\ell_d = \ell_{ds} \times N \ . \qquad (1)$$

Velocity was varied by adjusting the liquid supply pressure and, hence, the liquid flow rate. Initial droplet velocity, v_d, is given by

$$v_d = \ell_{ds} \times f_v \qquad (2)$$

where f_v is the vibrator frequency. The droplet generator assembly is mounted on a swivel fixture which permits a variation in the angle of injection of the droplets at a distance of approximately 14 cm from the burner axis.

Aerodynamic Flow Field Measurements

Radial profiles of temperature, velocity (three components) and species were measured at each axial position corresponding to the 5, 25, 46, 66 and 86 cm "radial sample ports" (Fig. 1), with confirming measurements of the 10 cm "axial sample port." Gas temperatures were measured by suction pyrometry; axial, radial and tangential velocity components were measured by using a specially designed five-hole pitot probe (water-cooled with 8 mm uncooled tip, calibrated). "Instantaneous" velocities of the

turbulent flow were recorded, allowing means and standard deviations to be calculated with a microcomputer. Consistency with overall mass balance was achieved to within 10 percent at each axial position.

Droplet trajectories were measured visually, with the aid of high speed photography.

EXPERIMENTAL RESULTS

In the cylindrical polar coordinate system used, x is the axial coordinate, r is the radial coordinate and θ is the angular coordinate, defined as zero in the horizontal plane and 90 degrees at the top of the combustor.

Type C Flame Characterization

A peak flame temperature of 1750 K was measured at the combustor centerline, near the tip of the visible flame, with temperatures decreasing to approximately 1100 K at the wall (Fig. 2). Axial symmetry was observed.

Figure 3 exhibits maps of the mean axial, radial and tangential velocity components in the near-burner zone. At each point there is actually a distribution of velocities over time due to turbulent fluctuations in the reacting flow. Standard deviations of velocity were in the range of 1 to 5 m/s, often 50 percent or more of the mean velocity. The axial velocity map (Fig. 3, top) shows strong internal recirculation within the flame (indicated by negative velocities), as well as external recirculation near the combustor walls. Peak velocities of greater than 25 m/s were measured near the burner quarl exit, consistent with the input

air velocity at the burner throat of 28 m/s. The calculated bulk mean axial velocity, approximately 2.6 m/s, is approached beyond the 50 cm axial distance.

Mean radial velocities were found never to exceed 8 m/s. Very little radial motion of the combustion gases was seen beyond the 25 cm axial location. Mean tangential velocities were found to be negative everywhere, consistent with the direction of swirl. A strong degree of swirl was observed near the burner quarl exit, with the swirl mostly dissipated by 40 cm downstream. The peak tangential velocity of approximately 12 m/s is consistent with a swirl number of 1.3.

Influence of Droplet Spacing on Coefficient: Cold Flow Conditions

It was hypothesized that droplet-to-droplet spacing would affect drag. Models that properly account for this phenomenon, in a three-dimensional external flow field, still remain to be developed. Therefore, in order to obtain data relating to a situation that could be modeled, it was necessary to determine the droplet spacing at which these aerodynamic interactions become negligible. Tests were performed to evaluate this effect in a nonevaporating, quiescent environment. A 210 μm droplet with an initial velocity of 7 m/s (Re=96) was aimed horizontally in a plastic tube. With no droplets removed, ℓ_{ds} = 510 μm, or 2.4 droplet diameters. The axial distance, L, for the droplets to fall a vertical distance, H, was measured for droplet spacing conditions of N = 1, 2, 4, 8, 16, 32, 64, 128, 256 and 512.

Neglecting drag in the vertical direction and assuming a constant drag coefficient, the force balance equations can be integrated over time to yield

$$L = \frac{4}{3} (\bar{C}_D)^{-1} \frac{\rho_\ell}{\rho_g} D \left[\ln\left(1 + \frac{3}{4} \bar{C}_D \frac{\rho_g}{\rho_\ell} \frac{v_d}{D} \sqrt{\frac{2H}{g}}\right)\right]. \quad (3)$$

Results (Fig. 4) show that $\bar{C}_D$, the mean drag coefficient, increases linearly with the logarithm of droplet spacing, until ln $(\ell_d/D) = 4.5$. For spacings of greater than 150 droplet diameters, $\bar{C}_D$ approaches 1.4. This value is in agreement with published values of C_D at Re = 96 for an isolated sphere.[13]

Droplet Trajectories: Hot Flow Conditions

Thirteen test conditions were evaluated, with droplet trajectories measured for variations in droplet spacing, velocity, size and injection angle. (See Table I.)

The domain of droplet trajectories observed for the nominal test condition is shown (Fig. 5) in the two planes of observation. Superimposed on the cross-sectional view along the centerline axis are lines of constant mean axial velocity of the combustion gases. The droplets were observed to follow an approximately common path until they entered the high shear layer of the combustion gas. This point, labeled IG, denotes the location of the earliest ignition point observed. The burning times were very short, and the burning droplet "flecks" lasted only over a few centimeters. The large shaded area denotes the distribution of burning droplets, igniting and burning out at various locations in this area.

Thus, there is no single trajectory that describes this test condition. The average burnout point of the droplets that penetrated axially the farthest is marked and labeled BO.

Mean droplet trajectories to the farthest droplet burnout point are shown in Fig. 6 for all 13 test conditions. Although these trajectories, which are based on measurement of IG and BO points, are somewhat qualitative, sufficient detail was observed for determining trends set by changes in the test parameters. It was observed that in all of the tests the droplets penetrated the flame zone. The flame length was between 10 and 15 cm, whereas none of the mean droplet trajectories was terminated before 20 cm. It was also observed that in most cases the droplets bypassed the flame.

In Fig. 6, the most closely spaced droplets (condition 2) are shown to penetrate farthest. Little effect of spacing is observed for values of greater than 20 diameters (conditions 1, 5 and 6). Axial penetration is shown to roughly double for a doubling of initial droplet velocity. Axial penetration increases as droplet diameter increases, as well. The effect of injection angle is observed for both the isolated droplet and the droplet stream. In these tests, almost no change in axial penetration distance is observed either for isolated droplet injection at 0, 30 and 45 degrees (conditions 12, 1 and 13, respectively) or for droplet stream injection at 0 and 30 degrees (conditions 11 and 2, respectively).

THEORETICAL MODEL

A simple numerical model to predict the trajectory of single droplets injected into swirled combusting flow fields was used to provide comparison with the experimental results and to guide future experimental efforts.

Description

The model is a direct adaptation of the numerical procedure developed by Ayers et al.[8] and is used to solve the uncoupled equations of droplet motion in a Lagrangian framework. A three-dimensional grid structure is established for specifying the (measured) background gas velocity, temperature and chemical speciation. Isolated, spherical, homogeneous droplets enter the computational domain at a specified position with specified (experimental) initial values for droplet diameter, temperature and velocity. The process is modeled in two steps: droplet heating to the liquid boiling point followed by droplet evaporation. Calculations are terminated when complete evaporation occurs, or when the droplet exits the computational domain.

Drag, calculated using an empirical coefficient[13], and gravitational forces are assumed to be the only external forces on the droplet. During droplet heating to the liquid boiling point, D is assumed to be constant (i.e., no evaporation), yielding

$$\frac{dT}{dt} = 6 \frac{Nu\lambda_g}{D^2 c_{p_\ell} \rho_\ell} (T_\infty - T). \qquad (4)$$

The Nusselt number is calculated using an empirical relation.[14] After the droplet temperature reaches the boiling point, evaporation begins:

$$\frac{dD}{dt} = -C_B \frac{1}{2D} (1 + 0.23\ Re^{0.5}) \qquad (5)$$

where the evaporation constant (C_B) depends on local gas properties.[15]

Four important limitations inherent in the model in its present form are:

1. Droplets are spherical, homogeneous and isolated.
2. The effect of evaporation on drag is not properly accounted for.
3. Radiation heat transfer to the droplet and heat generation due to chemical reactions are negligible.
4. Effects of turbulence in the combustion gases on droplet trajectories are not evaluated. Only mean trajectories are modeled.

Comparison with Data

For widely spaced droplets the predicted location at which the droplet is completely evaporated is compared to the experimentally measured range of droplet penetrations in Table I. Bounds on the experimental ranges at each test condition are given by the position of earliest droplet ignition and farthest droplet burnout. The model predicts only a mean evaporation point. No attempt was made to model the closely spaced droplets (conditions 2 through 6 and 11).

The model predicts an axial penetration near the experimental point labeled IG in all but the axial injection test (condition 12). Thus, it predicts a minimum axial penetration distance. The predicted radial location is in the experimental range for each condition. The predicted circumferential distance travelled is near the experimental point labeled BO in each test condition. Thus, the model predicts a maximum circumferential trajectory, apparently exaggerating the effect of swirl.

Predicted trends closely match those measured experimentally. Doubling the initial droplet velocity (4.9 to 9.1 m/s) approximately doubled the axial penetration (13.4 to 25.4 cm). Increasing droplet size increased the axial penetration. Finally, axial penetration of the 45 degree injection angle test (condition 13) was just slightly greater than the 30 degree injection angle test (condition 1). Considering the use of mean input values, agreement between the experimental and model results is good.

For the axially injected droplet, the predicted trajectory was much shorter than that measured. This may be due to the fact that droplet penetration is increasingly sensitive to relative droplet/gas velocity as the droplet evaporates, and, in the axial test (condition 12) near the combustor wall, gas velocities are very small (less than 5 m/s in magnitude) and the uncertainty relatively high. Additional model predictions, which utilized small adjustments in the gas velocity field near the wall (from -3 to +3 m/s), did closely match the axial penetration trend exhibited by the experimental data.

Prediction for Centerline Injection

In order to determine both the effect of centerline injection and the significance of rogue droplets, the model is further exercised, given the measured gas flow field. Two trajectories were calculated for each of two angles of injection: 0 and 45 degrees.

A droplet with a size (50 μm) and velocity (50 m/s) typical of mean droplets in actual sprays is considered first. The axial penetration is predicted to be 3.8 cm for the axially injected droplet and 4.5 cm for the droplet injected at 45 degrees. Therefore, both predictions indicate that this droplet would be evaporated in the flame zone.

Next, large rogue droplet (300 μm) trajectories are considered. In actual sprays, the large droplets would be expected to have velocities that are less than the mean, since the pressure drop across a nozzle is fixed. For a large droplet velocity set at 10 m/s, axial penetrations of 44.3 and 17.1 cm are predicted for the axially and 45 degree injected droplet, respectively. Thus, the large droplets with reduced velocities penetrate significantly farther than mean droplets.

DISCUSSION

Large droplet penetration and bypassing have been observed in both experimental tests and model calculations. This phenomenon, explained by the aerodynamics of large, single droplet combustion, would appear to be a potential cause of hazardous waste incinerator failure. The short burning distances and relatively

long trajectories of large droplets observed in the experiment suggest that droplet trajectory during heat-up and evaporation is primary, and gas phase combustion secondary, in understanding and predicting DRE.

It was experimentally observed that, in the initial portion of a large droplet lifetime, the droplet injection parameters dominate its trajectory. For a given size, spacing, velocity and injection angle, the droplets track an approximately common straight path until evaporation begins. Then, as the droplet size (and, thus, momentum) decreases, the turbulent gas flow field becomes increasingly dominant. Experimentally, this is observed in the distribution of droplet trajectories that describe a particular test condition after the first ignition point. Theoretical model calculations simulate these two modes as well. The rate at which the droplet approaches the gas velocity is a function of droplet size. Initially, the predicted droplet trajectory is insensitive to combustion gas flow field velocities. As evaporation occurs, however, sensitivity to gas velocity increases, and the droplet is transported by the mean gas flow field.

Lack of agreement between the experiment and model for the axially injected droplet near the burner wall has been attributed to uncertainty in the velocity field near the wall. Increased accuracy in the velocity measurement technique is necessary to evaluate this hypothesis.

Future model development must address two critical areas. First, both cold flow and hot flow experiments showed that droplet

spacing was a critical parameter in determining farthest penetration. Therefore, it is necessary to incorporate the functional relationship between drag coefficient and droplet spacing. The complexity of this problem is immense due to the fact that, in a practical combustor flow field, the drag force has components in three dimensions. Thus, the correction due to droplet spacing must include experimental correlations in three dimensions rather than the one-dimensional correlation derived in the cold flow tests described in this paper.

The second critical area to be addressed relates to the role of turbulent fluctuations in practical combustor flow fields. The model used in this paper predicts mean droplet trajectories using mean flow fields in swirling combustion environments. The experiments reported here have shown there is a need to model turbulence as well. One possible approach may involve use of a normal distribution of velocity fluctuations, based on measured mean and standard deviation values for gas velocity components. This will allow droplets to be tracked until evaporation and a distribution of trajectories to be described statistically.

The final product may then allow the role of rogue droplets on incinerator failure modes to be predicted.

NOMENCLATURE

C_B	evaporation constant
$\overline{C}_D$	mean drag coefficient
c_{p_ℓ}	liquid specific heat
D	initial droplet diameter
f_v	vibrator frequency
g	gravitational acceleration
H	vertical distance
L	axial distance
ℓ_d	droplet spacing after separation
ℓ_{ds}	droplet stream spacing
N	frequency divider
Nu	Nusselt number
Re	Reynolds number
t	time
T	droplet temperature
T_∞	combustion gas temperature
v_d	initial droplet velocity
ρ_ℓ	liquid density
ρ_g	local combustion gas density
λ_g	local combustion gas thermal conductivity

ACKNOWLEDGMENTS

The research documented in this report was conducted in the laboratories of the Combustion Research Branch of the U. S. Environmental Protection Agency's Air and Energy Engineering Research Laboratory at Research Triangle Park, NC. All financial support was provided by EPA.

REFERENCES

1. Chigier, N. and McCreath, C.G.: Acta Astronaut., 1, 687 (1974).

2. Kramlich, J.C., Heap, M.P., Seeker, W.R. and Samuelson, G.S.: Twentieth Symposium (International) on Combustion, (in press), The Combustion Institute, 1984.

3. Spalding, D.B.: Fourth Symposium (International) on Combustion, p. 847, The Combustion Institute, 1952.

4. Williams, A.: Combust. Flame, 21, 1 (1973).

5. Faeth, G.M.: Comb. Sci. Tech., 21, 123 (1977).

6. Law, C.K.: Prog. Eng. Comb., 8, 169 (1982).

7. Chiu, H.H., Ahluwalia, R.K., Koh, B. and Croke, E.J.: Spray Group Combustion. Paper presented at the Sixteenth Aerospace Sciences Meeting, Huntsville, Alabama, January 1978.

8. Ayers, W.H., Boysan, F. and Swithenbank, J.: Droplet Trajectories in Three-Dimensional Gas Turbine Flow Fields, Air Force Report AFOSR-TR-81-0543, September 1980.

9. Beér, J.M. and Chigier, N.A.: Swirling Jet Flames from an Annular Burner, International Flame Research Foundation, Doc. No. K20/a91, 1963.

10. Leuckel, W.: Swirl Intensities, Swirl Types and Energy Losses of Different Swirl Generating Devices, International Flame Research Foundation, Doc. No. G02/a16, 1968.

11. Sangiovanni, J.J. and Labowsky, M.: Combust. Flame, 47, 15 (1982).

12. Russo, R.E., Withnell, R. and Hieftje, G.M.: Appl. Spectrosc., 35, 531 (1981).

13. Dickerson, R.A. and Schuman, M.D.: Journal of Spacecraft and Rockets, 2, 99 (1965).

14. Ranz, W.E. and Marshall, W.R.: Chem. Eng. Prog., 48, 141, 173 (1952).

15. Wise, H. and Agoston, G.A.: Literature on the Combustion of Petroleum. American Chemical Society, Washington, D.C., 1958.

TABLE I

Comparison of model calculations with experimental results

Test Point No.	Test Variable	Droplet Injection Parameters				Experimental: IG/BO			Model Endpoint		
		Vel. (m/s)	Dia. (μm)	Spacing (μm)	Angle (deg)	Axial (cm)	Radial (cm)	Angle (deg.)	Axial (cm)	Radial (cm)	Angle (deg.)
1	nominal	7.0	210	510 x 64	30	15/45	7/15	335/245	21.8	10.2	238
2	spacing	7.0	210	510 x 1	30	35/75	8/25	240/200	-	-	-
3				x 2		30/65	5/23	240/200	-	-	-
4				x 4		10/55	6/20	330/250	-	-	-
5				x 8		10/45	6/18	330/240	-	-	-
6				x 16		25/40	8/11	270/260	-	-	-
7	velocity	4.9	180	340 x 64	30	15/25	5/10	330/270	13.4	7.7	253
8		9.1	210	640 x 64		30/60	8/15	300/225	25.4	10.4	242
9	size	8.5	250	620 x 64	30	35/60	8/13	270/225	32.6	12.5	228
10		8.5	315	615 x 64		45/70	10/20	270/225	49.0	16.4	212
11	angle	7.0	210	510 x 1	0	20/75	16/16	330/330	-	-	-
12				510 x 64	0	20/45	16/16	330/330	4.4	7.8	274
13				510 x 64	45	25/50	8/12	270/270	24.8	10.5	232

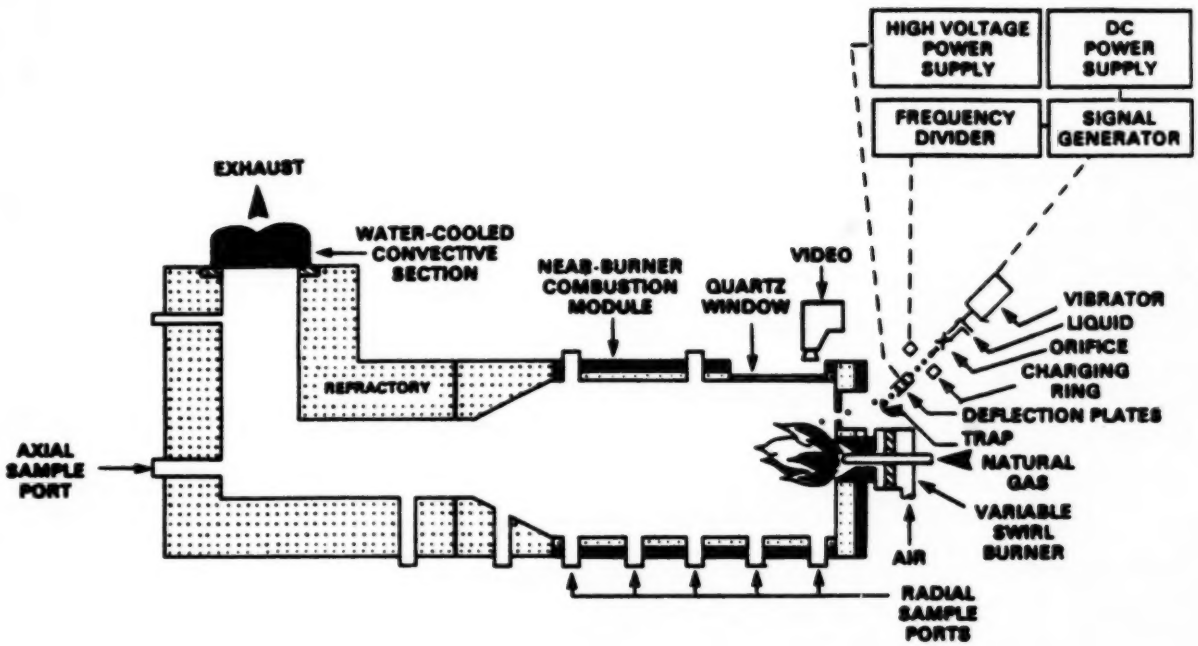

Figure 1. Schematic of bench-scale combustion facility. The 50 cm internal diameter, 90 cm long near-burner combustion module is water-cooled and insulated with a 4 cm thick refractory lining. The IFRF burner has a movable-block air swirl generator and interchangeable fuel nozzles. The monodisperse droplet generator is shown with electronics for droplet separation.

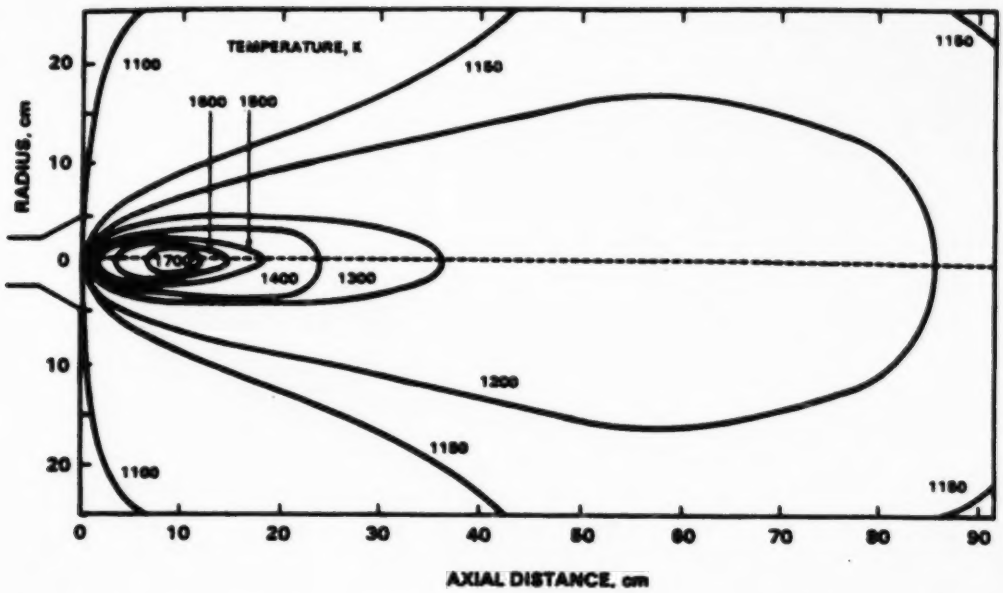

Figure 2. Near-burner zone isotherms for Type C flame baseline. This thermal map is constructed from axial and radial temperature profiles. Symmetry about the centerline axis was verified with a limited number of measurements and is assumed for the entire field.

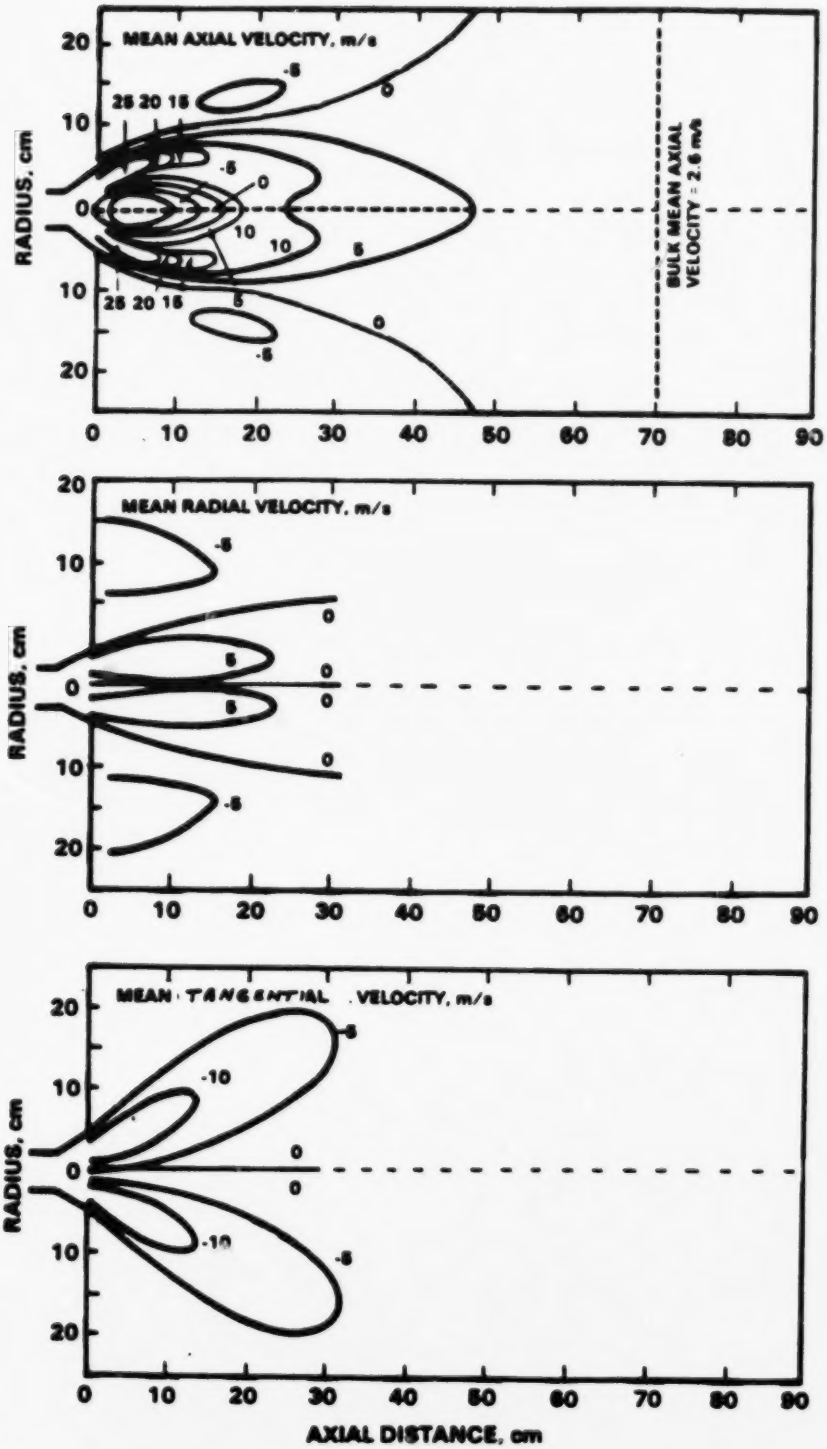
MEAN AXIAL VELOCITY, m/s
MEAN RADIAL VELOCITY, m/s
MEAN TANGENTIAL VELOCITY, m/s
RADIUS, cm
AXIAL DISTANCE, cm
BULK MEAN AXIAL VELOCITY = 2.6 m/s

Figure 3. Near-burner field axial, radial, and tangential velocity maps for Type C flame baseline. The lines of constant velocity are constructed from three-dimensional axial and radial velocity profiles. Symmetry about the centerline axis was verified and is assumed for the entire field.

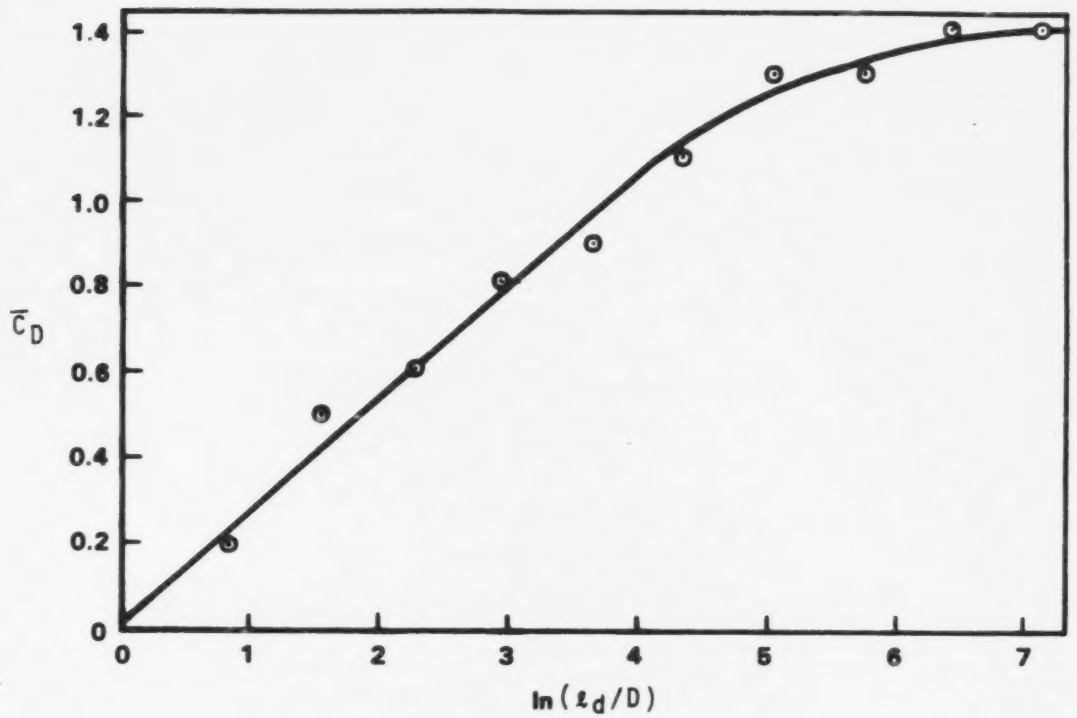

Figure 4. Mean drag coefficient, $\overline{C}_D$, as a function of droplet spacing for Re = 96. $\overline{C}_D$ is calculated using Equation (3).

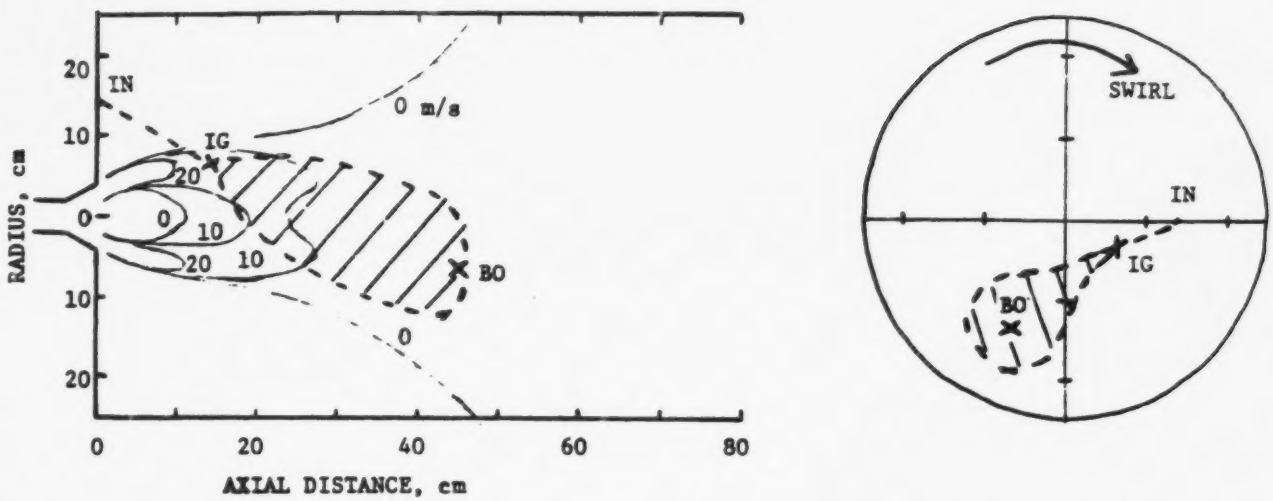

Figure 5. Droplet trajectories for nominal test conditions. The three-dimensional trajectories are shown in two plots: a top view and an end view. The domain of droplet burnout locations is shown by the shaded area. Axial velocity profiles are superimposed. The injection point (IN), the first ignition point (IG), and the last burnout point (BO) are noted.

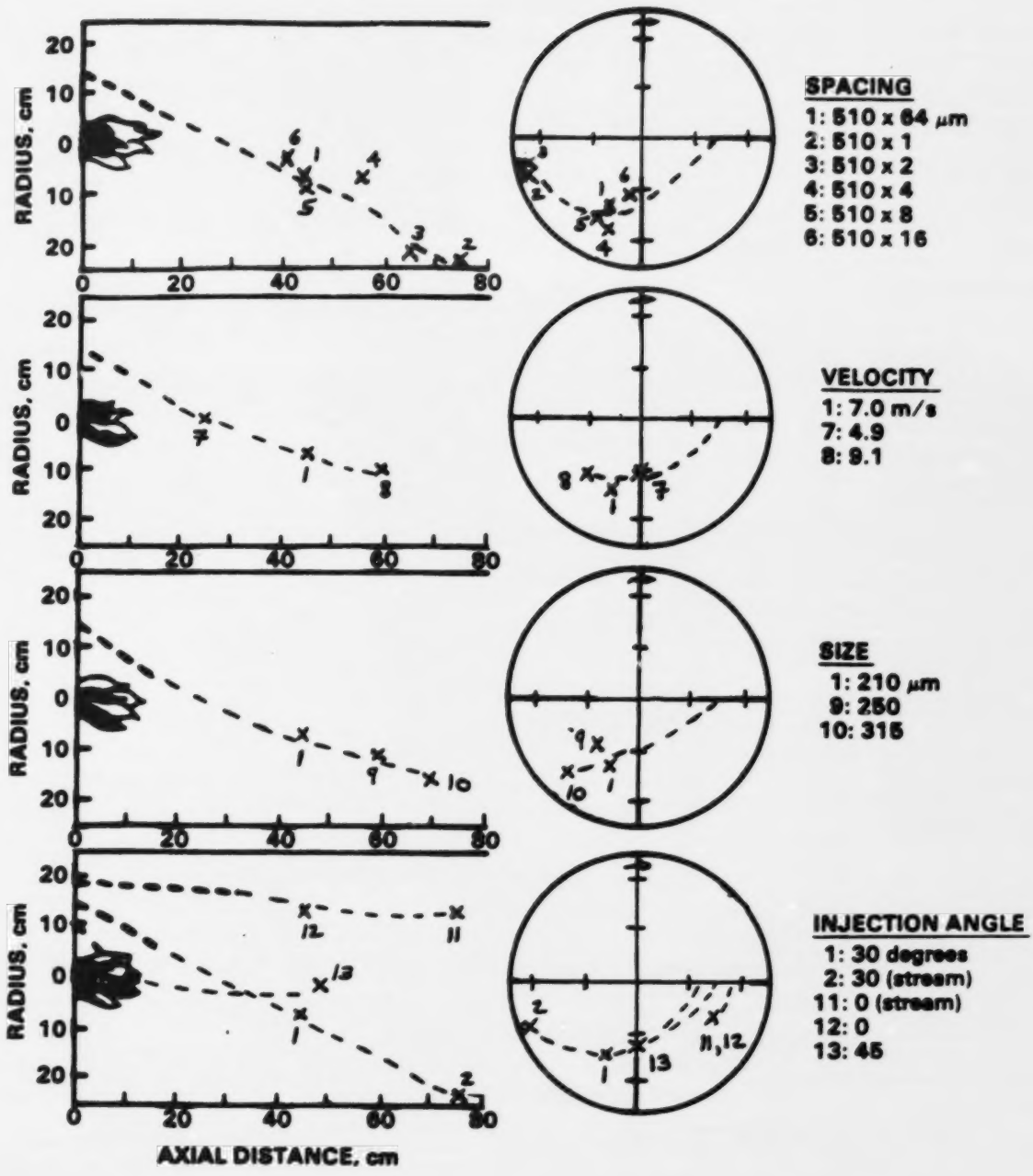

Figure 6. Mean trajectories to droplet burnout for 13 test conditions. A listing of the input droplet conditions is given in Table I. Each plot represents variation of a single parameter. From top to bottom, the variables are: droplet spacing, velocity, size, and injection angle. The droplet trajectory for test condition 1 is shown in each plot because it is the nominal test condition droplet path.